Measurements of Gamma-Ray Production Cross Sections of Nb and Cu for 15-MeV Neutrons

By

Kazuo SHIN and Tomoyuki ABE*

(Received July 3, 1989)

Abstract

Gamma-ray production cross sections of Nb and Cu are measured for 14.9-MeV neutrons. The accuracy of the experimental results is confirmed by comparing those with other experipental data obtained by similar energy neutrons. Hence, the data given in this paper are useful in the evaluation of secondary gamma-ray production data for fusion use.

Based on the measured data, some comments are given to the evaluated data in the ENDF/B-IV file: (1) the gamma-ray spectrum of Cu data is not adequate, (2) the gamma-ray yield data of the file for Nb is overestimated.

I. Introduction

Gamma-ray production cross sections for nominal 14-MeV neutrons are essential data for gamma-ray heating calculations in fusion neutronics design. Design studies on conceptual fusion reactors have been performed, using evaluated cross section files, mostly the ENDF/B-IV file[1]. However, the gamma-ray production data in the file are not always accurate enough to meet design criteria[2]. Continual efforts are required to improve the accuracy of the these data via new measurements.

A few works on systematic measurements of gamma-ray production cross sections for 14-MeV neutrons have been published[3-5]. The number of materials taken up in these works is still not enough. An attempt to make up a new Japanese evaluation of gamma-ray production cross sections requires more tests of already existing data in the ENDF/B-IV file.

Department of Nuclear Engineering, Kyoto University, Yoshida-honmachi, Sakyo-ku, Kyoto 606, JAPAN

* Power Reactor and Nuclear Fuel Development Corporation, Akasaka 1-9-13, Minato-ku, Tokyo 107, JAPAN

Previously, we reported the data for Ti, Ni and Mo[6]. In this paper, the measurement is extended to Nb and Cu. The objectives of the series of works are to systematically provide measured gamma-ray production data, and to make wide tests of the ENDF/B-Ⅳ evaluation based on the measured data.

Section Ⅱ describes the outline of the experimental method, and section Ⅲ the data reduction method. Results and discussions are written in section Ⅳ.

Ⅱ Experimental Method

Source neutrons were generated by D-T reactions, using a Cockcroft-Walton accelerator. The neutrons were injected into a sample of natural Nb or Cu. Secondary gamma rays following neutron reactions in the sample were detected by a 7.5-cm diameter by 7.5-cm long NE-213 scintillator.

Figures 1(a) and 1(b) show experimental arrangements for Cu and Nb, respectively. A 60-cm long iron shadow bar was placed between the T target

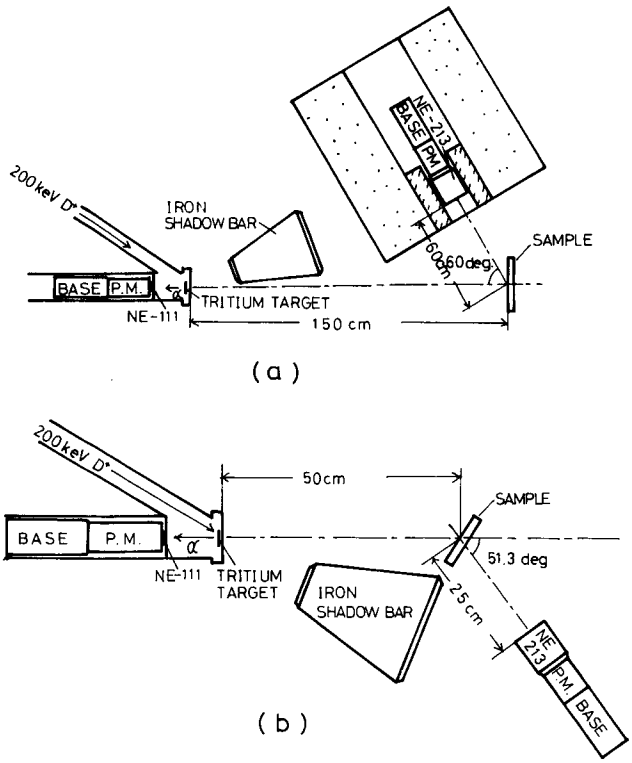

Fig. 1 Experimental arrangement.

and the detector to remove direct neutrons from the target.

The D^+ beam was collimated by a thin Cu-foil collimator to the 2.5-mm diameter. Alpha particles generated from the T target by D-T reactions were detected with a 0.1-mm thick NE-111 plastic scintillator through a 2-mm diameter window of a 1-mm thick Al foil. Neutrons (alpha-tagged neutrons) associated with the alpha particles emerged in the opposite direction to the alpha particle. The alpha particle beam was collimated, and the associated neutrons emerged within a sharp cone. The spread of the neutron beam was measured by a 1.25-cm diameter by 1.25-cm thick plastic scintillator. The neutron mean energy on the axis of the cone, determined by the TOF method, was 14.9 MeV.

The Cu or Nb sample was located in the cone of the alpha-tagged neutrons, so that the center of the sample came to the axis of the cone. The sample size is tabulated in Table I. The distance from the sample to the T-target was decided for most of the alpha-tagged neutrons to impinge to the sample, assuring enough space between the T-target and the sample to accommodata the iron shield. The iron shield was located carefully so as not to perturb the neutron beam.

An additional shield of concrete and lead was used in the Cu run (see fig. 1 (a)) as a detector shield for both of the direct neutrons from the target and background neutrons. As the size of the Nb sample was samller, the NE-213 scintillartor was moved closer to the sample in the Nb run. Hence, there was no space to set the additional detector shield in the Nb run. The detector was located, without the shield, at the opposite side of the sample to the T target to minimize the influence of the direct neutrons on the detector by maximizing the distance from the target.

Fig. 2 shows the block diagram of the measuring system. The NE-213 scintillator detects gamma rays exclusively by discriminating neutrons with the aid of an n-γ discrimination circuit. The time discrimination technique of the associated particle method[7] is utilized to help the selection of desired gamma-ray events from background events.

Table I Dimensions of Nb and Cu Samples Used in the Measurement

Sample	Diameter (cm)	Thickness	
		(cm)	(mfp)[a]
Nb	9.3	2.0	0.435
Cu	15.0	1.5	0.359

[a] Mean free path for 15-MeV neutrons.

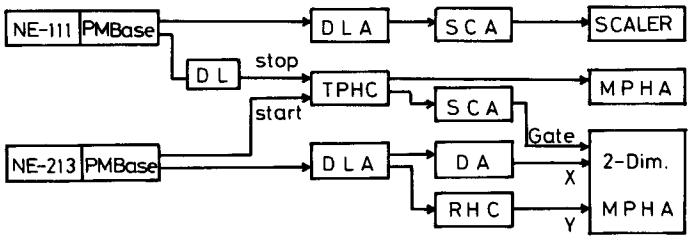

Fig. 2 Blockdiagram of the measuring system. PM-Base is a constant fraction timing photomultiplier tube, DLA is a delay line amplifier, TPHC is a time to pulse height converter, SCA is a single channel analyzer, RHC is a rise time to height converter, DA is a delay amplifier, and MPHA is a multichannel pulse height analyzer.

Ⅲ Data Reduction

The measured gamm-ray pulse-height spectra were unfolded to the energy spectra with the FERDO[8] code, using the response functions calculated by the Monte Carlo method[9]. The response functions have been applied to a variety of gamma-ray fields, and the accuracy has been confirmed. Other procedures used to obtain the cross-section values are described below.

(1) Estimation of the Number of Neutrons Incident to the Sample

The number of neutrons incident to the samples were determined as the product of the total counts of alpha particles detected by the NE-111 scintillator and the probability that alpha-tagged neutrons hit the sample.

Fig. 3 shows the pulse-height spectrum of the NE-111, in which a peak is ascribed to alpha particles. The total alpha count was the difference between the area of the peak region and the background which was estimated by extrapolating the background spectrum in the lower pulse-height region to the peak region with a fitted exponential curve.

Fig. 4 shows a count rate profile of alpha-tagged neutrons for the geometry of Fig. 1(b) (Nb run). The profile was measured with a 1.2-cm diameter by 1.2-cm long plastic scintillator at the sample position on a plane perpendicular to the neutron beam axis. The neutron flux profile was obtained from the count-rate profile as follows. A trial neutron flux profile was assumed and integrated over the detector area to generate a count-rate profile, which was then compared with the measured one. The process was repeated until a satisfactory profile, shown by a solid line in the same figre, was obtained.

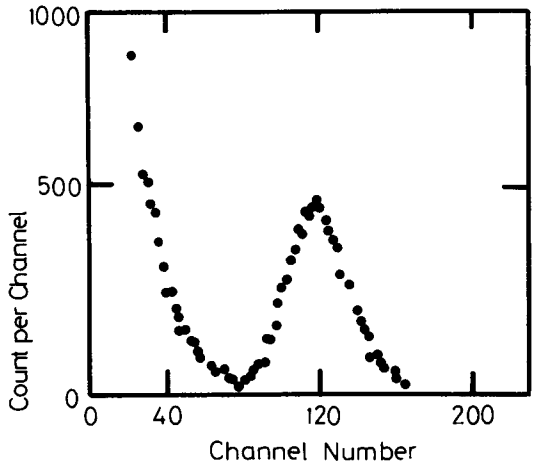

Fig. 3 An example of the pulse-height spectrum of the alpha-particle detector.

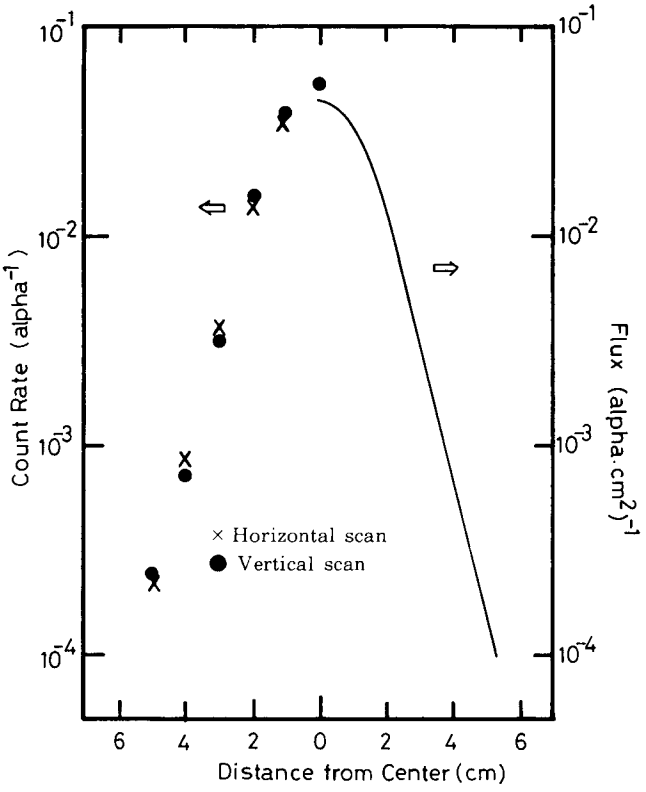

Fig. 4 Count-rate profile of alpha tagged neutrons in the cone obtained with the 1.2-cm diameter by 1.2-cm long plastic scintillator.

The probability that the alpha-tagged neutron hit the sample was calculated from the neutron-flux profile to be 0.98 for the Nb sample. The same process was used for the Cu target, and the probability was 0.78.

(2) Depression of Source Neutron Flux in Sample

The average source-neutron flux in the sample was necessary to convert measured data to cross sections.

Source neutrons produce mostly elastic and inelastic scattering, and (n, 2n) reactions in the sample. Here, we assumed that the neutron-energy change in the elastic scattering was negligible, while secondary neutrons from non-elastic scattering were ignored. Then the elastic scattering did not contribute to the flux depression of the source neutrons, and the average flux depression rate in the sample was given by the following equation:

$$p=\frac{1}{a}\int_0^a e^{-\Sigma_n t}\,dt=\frac{1-e^{-\Sigma_n a}}{\Sigma_n a}, \tag{1}$$

where $a=t_0/\cos\theta$,

t_0=sample thickness,

θ=neutron incident angle to the sample,

and Σ_n=non-elastic cross section of the sample.

The calculated values of p were 0.09 for both samples.

The assumption made above is slightly rough. Some of the secondary neutrons from the non-elastic collisions still maintain enough energy to generate a similar amount of gamma rays to the amount by source neutrons. If the assumption is made that all the secondary neutrons contribute to the production of gamma rays at the same rate as do the source neutrons, the neutron flux in the sample should be 1.05. If this is the case, the use of 0.09 as the flux depression rate may result in a 15% overestimation at maximum to the gamma-ray production cross section.

(3) Self-Shielding Effect of Sample to Secondary Gamma Rays

The self-shielding effect of the sample on gamma rays which were emitted from neutron reactions in the sample to the detector direction was estimated simply by the attenuation of these gamma rays in the sample, i.e. by the simple attenuation law without a buildup correction. The equation used for this purpose is

$$\gamma(E_\gamma)=\frac{\int_0^{t_0} e^{-\Sigma_n l}\cdot e^{-\mu(E_\gamma)\frac{x}{|\cos\varphi|}}\,dt}{\int_0^{t_0} e^{-\Sigma_n l}\,dt}, \tag{2}$$

The quantity $\mu(E_\gamma)$ is the linear-attenuation coefficient for gamma rays of the energy E_γ, φ is the gamma-ray emission angle, and l and x are given by,

$$l=\begin{cases} t & \text{(Cu sample)} \\ t/\cos\theta & \text{(Nb sample)}, \end{cases}$$

$$\text{and } x=\begin{cases} t & \text{(Cu sample)} \\ t_0-t & \text{(Nb sample)}. \end{cases}$$

Since gamma rays lose a large amount of their energy by a single scattering, the buildup effect of gamma rays, which was neglected in the above estimation, affects only a very low energy part of the spectrum.

(4) Estimation of Background

The background gamma rays were composed of two components, i.e. time-independent and time-dependent components.

The time-independent background was due to the random coincidence of NE-213 events with NE-111 events. Therefore, it was proportional to the square of the total neutron yield. The shape of the gamma-ray pulse-height spectrum due to this background component was determined by a special run without the sample, where the D^+-beam current was increased to obtain a much larger neutron yield than in the normal run, so that in the NE-213 events the time-dependent background was negligible. The absolute value of this spectrum was evaluated by using counts of the flat part in the time spectrum obtained in the normal run with the sample.

The time-dependent component is classified into two types; one is due to the interaction of alpha-tagged neutrons with the sample support or the shield. The other is the double interaction of those neutrons or gamma rays with the sample first and then with the support or the shield. In the second case the interaction could occur in the reversed order, i.e. first in the support or the

shield then in the sample, or twice with materials other than the sample.

The determination of the time-dependent background component, in which the interaction with the sample is involved, is not possible by the experiment. However, since the occurrence of the double scattering is not frequent as compared with the single scattering, the first type component seems dominant. Hense, the time-dependent background was important in the Cu run, because 22% of the alpha-tagged source neutrons missed the sample.

The amount of this background component was determined from a pulse-height spectrum measured in a special background run with the normal D^+ -beam current .and the normal time gate but without the sample. The time-independent background component was subtracted from the obtained spectrum by using the flat part in the time spectrum of this run.

(5) Error Estimation

Errors due to the correction of the background in the alpha counts were considered to be less than 5%. The estimation for the spill of source neutrons out of the sample contained about a 3% error.

It was assumed in the evaluation of the depression of the source-neutron flux in the sample that the secondary neutrons generated by the non-elastic scattering in the sample generated no more secondary gamma rays. If this was not the case, the above estimation would cause a 15% error at maximum including the two neutron emissions from the (n, 2n) reaction.

An error estimation for the gamma-ray self shielding effect in the sample was not performed.

The errors introduced in the unfolding process were estimated by the method proposed by Shin et al[10]. The estimation included errors due to the response functions, to statistics in the pulse-height spectrum and to the step-function approximation of the response function and pulse-height spectrum.

The sum of these errors was used for the total estimated errors in the final cross section values.

IV Results and Discussions

The measured gamma-ray spectra were converted to double differential cross sections $d^2\sigma/dE_\gamma d\Omega$ for the secondary gamma-ray production by 14.9-MeV neutrons.

Fig. 5 shows the result for the Cu sample. The experimental result by Dickens[11], obtained for neutrons in the energy interval of 14-17 MeV, and the

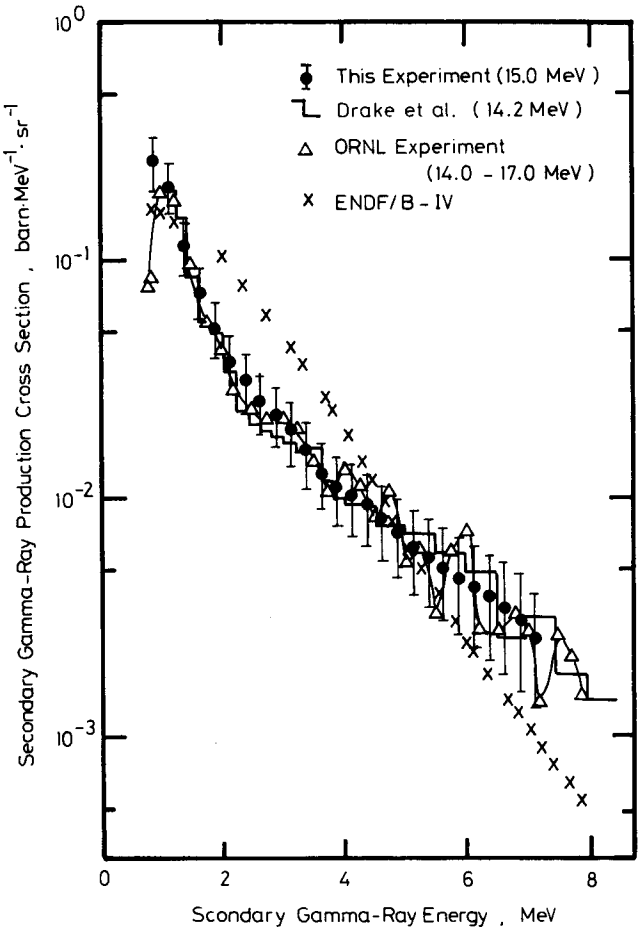

Fig. 5 Comparison of differential gamma-ray production cross section data of Cu, among our work, Dickens' experiment[11], Drake's measurement[4], and ENDF/B-IV data.

other one given by Drake[4] for monoenergetic neutrons of 14.2 MeV are also shown together in the same figure for a comparison with our results. These three results are in good agreement with one another over the whold energy range.

As the accuracy of the measured data is confirmed, the evaluation by the ENDF/B-IV is tested by the measured values. The evaluated data for the secondary gamma-ray production cross sections for the 15.5-MeV neutrons are cited in the same figure from the ENDF/B-IV file. The data of the ENDF/B-IV are very different from the experimental values.

The angular correlation of the gamma-ray yield is usually very weak. We assumed the isotropic distribution of the gamma-ray emission. The values in

Table II Secondary Gamma-Ray Yield Integrated above 1-MeV Gamma-Ray Energy

Data	Secondary Gamma Ray Yield (barns)	
	Nb	Cu
This Work	1.35	2.37
Drake et al.	1.64	1.834
Dickens et al.	2.309	2.069
ENDF/B-IV	3.303	1.793

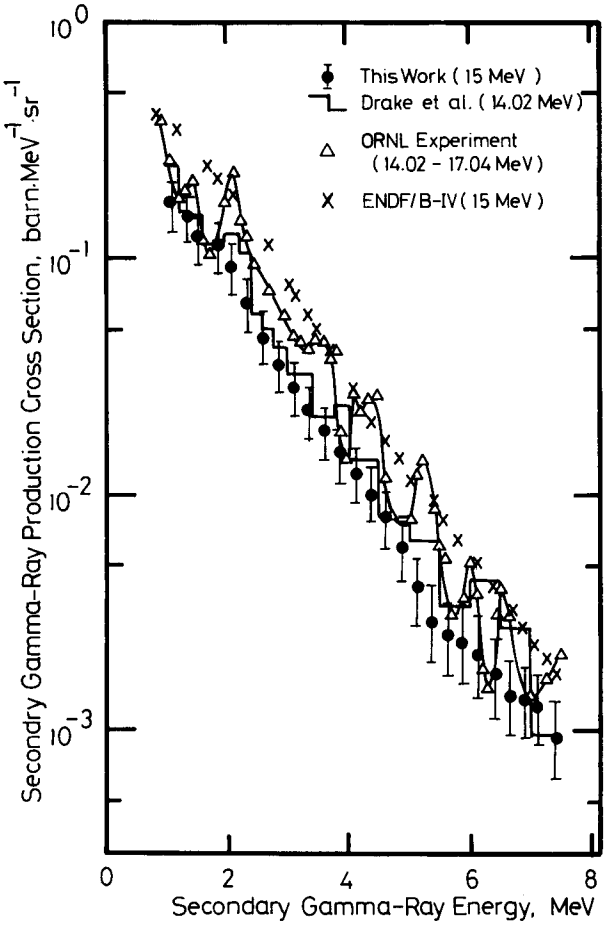

Fig.6 Comparison of differential gamma-ray production cross section data of Nb, among our work, Dickens' experiment[12], Drake's measurement[4], and ENDF/B-IV data.

Fig. 5 were integrated over the gamma-ray energy range above 1 MeV and were multiplied by 4π to yield the total gamma-ray yield. The results are tabulated in Table II. The ENDF/B-IV data agree very well with the data by Drake, while our data are a little higher than others. This is due to the rise at the lowest energy bin in our spectrum. The reason for this rise is still not clear. It may be due to the poor n-γ discrimination performance at a very low pulse-height and to the buildup of scattered gamma rays caused by the self-scattering in the sample.

Fig. 6 shows the gamma-ray production cross section of Nb. Our result is close to that by Drake[4]. However, our values are systematically smaller than Drake's data. The values by Dickens[12] are higher than these two experiments. As for the evaluated data by the ENDF/B-IV, it is seen in the figure that the data are much higher than any of these experimental values.

The gamma-ray yield from Cu is similarly shown in Table II with other experimental results and the ENDF/B-IV data. The ENDF/B-IV data are much higher than the experimental values.

V Conclusions

The differential gamma-ray-production cross-section data of Cu and Nb for 14.9-MeV neutrons were presented.

From the comparison of our results with other experiments and the ENDF/B-IV data, the following was found out for the evaluated data in the ENDF/B-IV. (1) The spectrum of gamma rays for Cu was very different from those of the experiments. (2) The gamma-ray yield data for Nb were overestimated.

Acknowledgement

Valuable discussion with Prof. T. Hyodo is gratefully acknowledged.

References

1) "ENDF/B Summary Documentation for ENDF/B-IV," ENDF-201 (ed. R. Kiney), available from the National Nuclear Data Center, Brookhaven National Laboratory.
2) M. Abdou et al., "FINESSE: A Study of the Issues, Experiments and Facilities for Fusion Nuclear Technology Research and Development," PPG-821, University of California, Los Angeles (1985).
3) G. L. Morgan and F. G. Perey, Nucl. Sci. Eng., 61, 337 (1976).
4) D. M. Drake, Nucl. Sci. Eng., 40, 294 (1970). ; see also Nucl. Sci. Eng., 65,49 (1978).

5) V. J. Orphan et al., Nucl. Sci. Eng., 57, 309 (1975).
6) K. Shin et al., J. Nucl. Sci. Technol., 17, 531 (1980).
7) G. C. Bonazolla et al., Nucl. Instr. Methods, 70, 137 (1969).
8) W. R. Burrus and V. V. Verbinski, Nucl. Instr. Methods, 67, 181 (1969).
9) K. Shin et al., J. Nucl. Sci. Technol., 16, 390 (1979).
10) K. Shin et al., Nucl. Technol., 53, 78 (1981).
11) J. K. Dickens et al., "Gamma-Ray Production Due to Neutron Interactions with Copper for Incident Neutron Energies between 1.0 and 20 MeV," ORNL-4846, Oak Ridge National Laboratory (1973).
12) J. K. Dickens et al., "Nb(n, xγ) Reaction Cross Section for Incident Neutron Energies between 0.65 and 20 MeV," ORNL-TM-4972, Oak Ridge National Laboratory (1975).